JJMIE

Volume 18, Number 4, December. 2024
ISSN 1995-6665
Pages 861- 875
https://doi.org/10.59038/jjmie/180417
Editor-in-Chief: Prof. Ali M. Jawarneh

Jordan Journal of Mechanical and Industrial Engineering

Designing Optimal Parameters Using Taguchi Method for the Tribological Analysis of Al-Si alloy (LM29) Reinforced with Multi-Walled Carbon Nanotubes via the Liquid Metallurgy Route

Vikram Kedambadi Vasu[1], Umashankar K S[2], Vijay Kumar S[*3], Hanamantray Gouda M B[4], Jyothi A M[5], Chethan D[6], Vijee Kumar[7]

[1]*Department of Mechanical Engineering, Nitte Meenakshi Institute of Technology, Yelahanka, Bengaluru, Visvesvaraya Technological University, Karnataka, India.*
[2]*Department of Mechanical Engineering, KVG College of Engineering, Sullia, Dakshina Kannada, Karnataka, India.*
[3] *Centre for Robotics Research and Department of Mechanical Engineering, Nitte Meenakshi Institute of Technology, Yelahanka, Bengaluru, Karnataka, India.*
[4] *Department of Mechanical Engineering, Sir M Visvesvaraya Institute of Technology, Bengaluru, Karnataka, India.*
[5]*Department of Mathematics, Bangalore Institute of Technology, K R Road, V V Pura, Bengaluru, Karnataka, India.*
[6]*Department of Mechanical Engineering, B M S Institute of Technology and Managament, Yahanaka, Bangalore-560064.*
[7]*School of Mechanical Engineering, REVA University, Yelahanka, Bengaluru, Karnataka, India.*

Received 29 Jul 2024 *Accepted 13 Oct 2024*

Abstract

The current research looks into the aluminum-based metal matrix nanocomposites tribological behavior fabricated using the Stir Casting Method. Multi-walled Carbon Nanotubes (MWCNT's) are used as reinforcements to improve the quality of metal properties and reduction in wear rate. In the current work, the metal matrix Aluminum alloy (LM29) was chosen to be reinforced with MWCNTs (with 0.25 wt%, 0.50 wt%, and 1.00%) to produce Metal Matrix Nanocomposites. A computerized pin-on-disc setup was used to conduct the entire tribological experiment, with input variables including the MWCNT composition (0.25%, 0.50%, 1.0%), cooling method and stirring speed (250, 450, and 650rpm), all while maintaining a constant load of 20 N. The observations are created using Taguchi (L9) orthogonal array, which is one of the most reliable methods. In comparison to compositions, ANOVA revealed that sliding distance is the most adaptable factor. All of the tests were conducted with a constant load of 20 N, and ANOVA showed that the kind of cooling is the most important element. Finally, worn-out regions of the specimens were examined using scanning electron microscopy (SEM), and the value of the regression equations was assessed using a confirmation test. For all the combinations considered, the confidence interval 95% with a error of 5% was achieved.

© 2024 Jordan Journal of Mechanical and Industrial Engineering. All rights reserved

Keywords: LM29, MWCNT's, Wear, Taguchi, ANOVA, SEM.

1. Introduction

Because of its small weight, aluminum allows for weight savings. Due to this metal's brittle nature, its applicability in engineering may be limited. Because high strength-to-weight ratios are required in the civil and military sectors for rockets, missiles, aircraft structures, and light armoured vehicles, this metal must be strengthened before it can be used in these applications. Usually, Cu, Zn, Mn, Mg, Si, and Li are alloyed with Al to reinforce it, and the alloys are then heated. [1]. Aluminum has a density of 2.7 grammes per cubic centimeter, which is roughly one-third that of steel (7.83 grammes per cubic centimeter). Approximately 490 lb (222 kg) of steel is contained in a cubic foot of steel, while 77 kg (170.7 lb) is contained in a cubic foot of aluminum. In addition to its lightweight, some aluminum alloys are relatively strong (exceeding that of structural steel) and are widely used for the design and construction of strong, lightweight structures, such as aircraft and spacecraft.

Recent advancements indicate that the vehicle's body weight can be reduced by up to 30% through the substitution of steel with aluminum. Researchers are particularly interested in investigating the tribological properties of hyper-eutectic Al-Si alloys (LM29), which are extensively utilized in automotive engine components subjected to constant sliding wear. According to a parametric study of the effect of silicon morphology on Al-Si alloy wear rates and transition loads, the morphology of silicon has both a positive and a negative effect [2-5]. As a function of silicon,

* Corresponding author e-mail: vijaysnitk@gmail.com.

 © 2024 Jordan Journal of Mechanical and Industrial Engineering. All rights reserved - Volume 18, Number 4 (ISSN 1995-6665)

wear rates did not follow a consistent trend in binary unmodified Al-Si alloys. Furthermore, as silicon content increased in spray-produced Al-Si alloys, the wear performance improved [6]. Despite this, no comprehensive analysis of the tribological characteristics of hypereutectic aluminum-silicon alloys (LM29) exists. This paper investigates the wear properties of hypereutectic Al-Si alloys with a variety of compositions [10].

Recently, the Taguchi approach was used to do an efficient study of a complicated system [11]. The Taguchi method involves the following steps: identifying manageable issues and their stages; identifying unmanageable issues and assessment settings; designing a Taguchi crossed array design; conducting experimentations under experimental settings; analyzing outcomes; determining the optimal run; and confirming the optimal run [12-17]. The challenge in optimizing a CNT synthesis stems from a lack of awareness of the true causative and individual product relationship. Multiple linear regression analysis can be used to anticipate response variables when there is no clear relationship between response variables and cause factors [18-20].

The fabrication of aluminum nanocomposites with various percentages of MWCNTs by stir casting is considered in this study. The main contribution of this study is the optimization of tribological properties of LM29 reinforced with MWCNT using the Taguchi method. This distinguishes the work from others by focusing on wear rate reduction. By applying optimum synthesis conditions, the Taguchi design technique is applied to optimize the process and manufacture a standard carbon nanotube in a number of ways. As a cost-effective and efficient approach, a prediction model is also being developed for CNT synthesis. Finally, statistical analysis was carried out to validate the results of the experimental results.

2. Materials and Methods

2.1. Materials

The matrix used in this research activity is Al-Si (LM29), which was purchased from Fenfee Technologies in Bengaluru, Karnataka. Table 1 displays the weight percentages of Aluminum and Silicon from the EDS Spectra. From this table value, we can get the varied wt. percent composition of Si combined with the matrix Aluminum. An electron beam is swept through a specified spot at particle matrix interface of Al-Si composite (LM29) (LM29). The figure 1 (a) displays the colored SEM micrographs of LM29 Alloy examined at specific location in the specimen and figure 1 (b) shows the EDS spectra at the chosen Area 1.

2.2. Multi-Walled Carbon Nanotubes

Carbon nanotubes (CNTs) are nanomaterials composed entirely of carbon. This study focuses on multi-walled carbon nanotubes (MWCNTs), which hold significant industrial relevance and were sourced from AdNano Technologies in Hassan, Karnataka. Essentially, MWCNTs fulfill three critical industrial properties: electrical conductivity (comparable to copper), mechanical strength (5 times stronger than steel while being 5 times lighter), and thermal conductivity (four times stronger than copper and five times more efficient than diamond). In combination, these remarkable properties can be applied in a wide variety of helpful and beneficial ways. MWCNTs are used as reinforcements, and their properties are listed in Table 2, along with TEM and SEM images in Figure 3 and XRD profile of the MWCNTs as received in Figure 4.

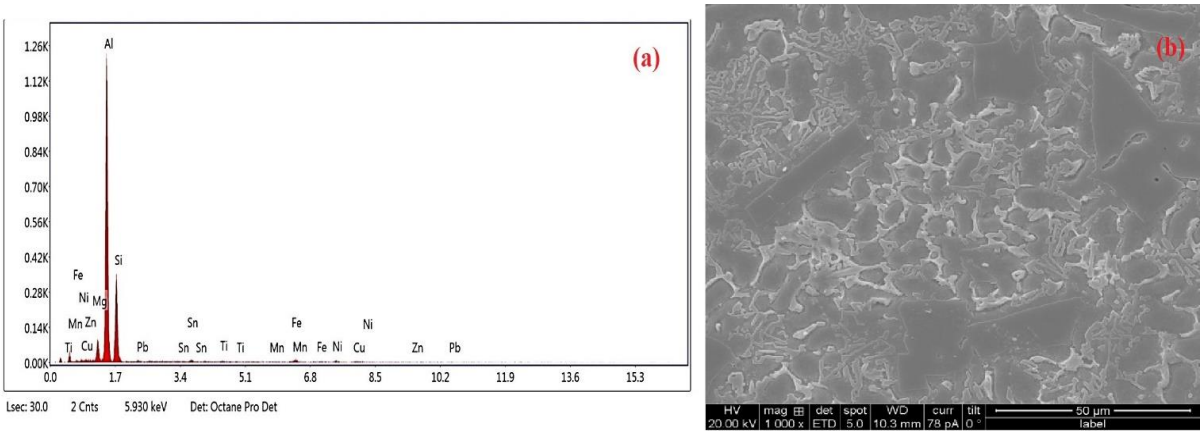

Figure 1. (a) EDS spectra at the selected Area of Specimen, (b) SEM micrograph of LM29 Alloy of Specimen

Table 1. Percentage of Elements of LM29 Aluminum alloy

Elements	Cu	Mg	**Si**	Fe	Mn	Ni	Zn	Pb	Sb	Ti	**Al**
Percentage (%)	0.1	0.1	**12.8**	0.6	0.5	0.1	0.1	0.1	0.1	0.05	**Rest**

Table 2. Properties of MWCNT

Property	Purity	L * D	Strength	Surface Area	Melting Point	Density
Values	Carbon >99%	2.5µm * 8 nm	45 Gpa	370 m^2g	3645°C	~2.1 g/ml at 25 °C

The X-ray diffraction (XRD) profile of multi-walled carbon nanotubes (MWCNTs) shows a distinct peak at a 2θ position angle of 28º. This peak stands out in the XRD spectrum, with counts exceeding 4000 across a phase shift range of 0º to 90º. Such a characteristic peak is primarily attributed to the spiral and helical structure inherent in multi-walled carbon nanotubes. Three alternative reinforcement and matrix compositions were evaluated for different compositions considered and is given in Table 3 and shown in Figure 5.

Table 3. Composition of Reinforcements

Aluminum Matrix Nanocomposites (AMNC)	Composition
AMNC (A)	LM29 + 0.25% of MWCNT's
AMNC (B)	LM29 + 0.50% of MWCNT's
AMNC (C)	LM29 + 1.00% of MWCNT's

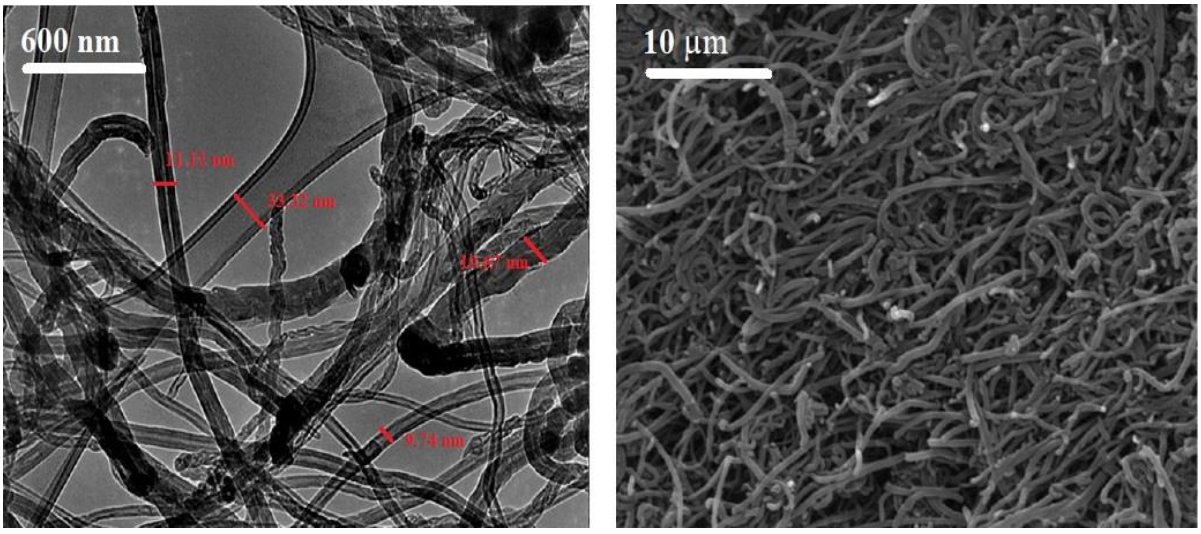

Figure 3. TEM and SEM micrographs recorded on the MWCNT's

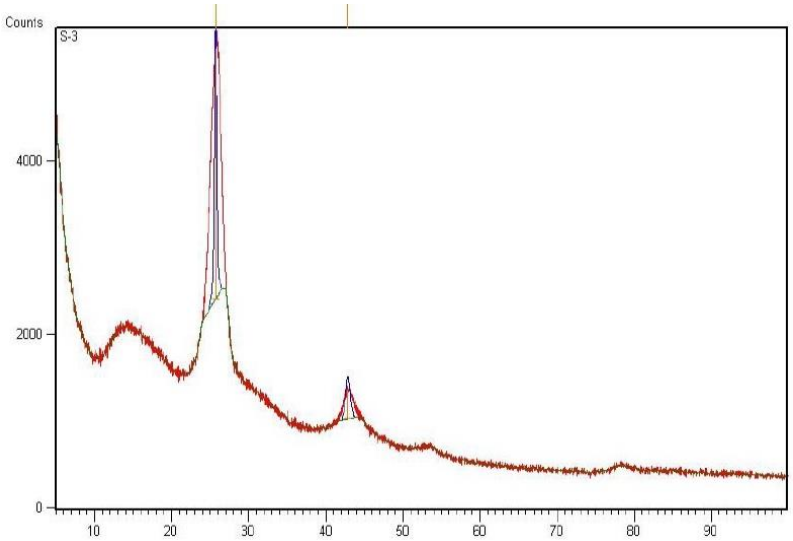

Figure 4. XRD profile of as received Multi Walled Carbon Nanotubes

Figure 5. (a) As-Cast Ingot of LM29 Alloy and (b) As-received Multi Walled Carbon Nanotubes

 © 2024 Jordan Journal of Mechanical and Industrial Engineering. All rights reserved - Volume 18, Number 4 (ISSN 1995-6665)

2.3. Method - Preparation of Metal Matrix Nanocomposites

The stir casting process is employed to incorporate varying percentages of multi-walled carbon nanotubes (MWCNTs) as reinforcement into the LM29 aluminum alloy. Ingots are procured and accurately cut to the required quantities using a power hacksaw. The metal matrix and reinforcement materials are weighed precisely on a scale. Since aluminum has a melting point of 660°C, the mixture is mechanically stirred for 30 minutes while heating the aluminum ingots to 700°C to ensure uniform dispersion. Initially, an emulsion is prepared by mixing 16 grams of MWCNTs with 150 ml of acetone as the dispersion medium in a beaker at room temperature. This mixture is stirred for about 15 minutes at 1000 rpm to achieve uniform dispersion. In a separate beaker, a mixture comprising 2 grams of sodium lauryl sulfate (a dispersant for nanotubes), 2 grams of Tween 80 (an emulsifier), and 25 ml of acetone is gently swirled for 15 minutes at 1000 rpm at room temperature to ensure the uniform dispersion of the nanotubes within the metal matrix. Then, this mixture is combined with the nanotube-containing liquid in a single beaker to generate the MWCNT emulsion. To prevent agglomeration and ensure a homogeneous mixture with aluminum, the MWCNT emulsions are preheated to 90°C in a pit furnace.

Manual stirring for 5 minutes, and mechanical stirring for 10 minutes are required during the pouring procedure. To improve the composite wettability, 1 weight percent magnesium is added to the matrix and reinforcement. Each casting product has different reinforcements and a different preparation to produce after this procedure is repeated nearly three times. Shielding gases such as nitrogen and argon are used in this process to prevent oxidation of the molten metal. In order to prevent gas buildup in the castings, the bottom pit is then opened and the slurry is slowly poured into the mold in a continuous flow. The mold is allowed to cool completely for thirty minutes after that, at which point the specimens are removed to finish the chilling process. The specimens are then sliced for wear testing in compliance with ASTM guidelines.

2.4. Wear Test

An EN32 steel disc was used for sliding wear tests in a pin-on-disc wear testing apparatus with a ASTM G99, with a constant weight of 2 kg and a sliding speed of 1 m/s. The pin's diameter and length were each 8 mm. A piece of emery paper was used to roughen the surfaces of the pin samples before testing. The fresh sample was slid over 240-grit emery paper to ensure that the new surface would effectively contact the steel disc. By bringing the specimen into close contact with the revolving disc, the specimens are loaded with a cantilever mechanism as they slide. Each sample was weighed using a microbalance and cleaned with acetone both before and after testing. Weight loss and sliding distance were used as the factors to compute the wear rate, which was expressed as volume loss per unit sliding distance.

Figure 6. (a) Stir Casting Setup, (b) Poured Specimen, (c) Allowed to Cool, (d) Final Specimen

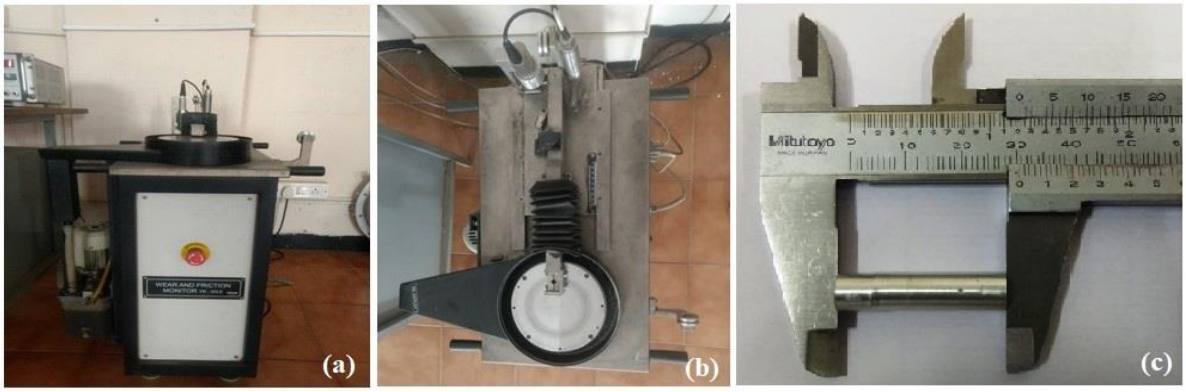

Figure 7. (a) Front View and (b) Top view of the Pin on Disc Setup and (c) Specimen for Pin on Disc experiment

50mm

The specific wear rates for the materials were determined via

$$W = \Delta w / L\rho F \quad (1)$$

W is the wear rate in mm^3/N-m, *w is the weight loss in g, L is the sliding distance in metres, D is the worn material density in grams per millimeter, and F is the applied load in N. The figures 8 and 4 show the weight loss of alloy and composite samples, and the setup parameters for pin on discs are shown in Table 4. The figure 8 shows a bar graph comparing the wear loss in grams of various specimens of LM29 alloy with varying percentages of MWCNTs (Multi-Walled Carbon Nanotubes) reinforcement. Thus, the addition of MWCNTs generally reduces wear, with 0.50% MWCNTs being the most effective in minimizing wear loss.

Table 4. Wear Parameters

Length (mm)	Diameter (mm)	Velocity (m/s)	Track Dia (mm)	Weight (kg)	Time (sec)
50	8	1.6	60	2	1800

3. Results and Analysis of Wear Rate

3.1. Factor Selection and Interaction

The responses of interest are used to determine which factors to explore. Cause and effect analysis, brainstorming, and pilot experiments were used to identify the components for the current research work. LM29 is the matrix chosen for the current study and the parameters varied were the compositions of reinforcements MWCNT's (0.25%, 0.50% and 1.00%), and the second factor was the type of cooling in terms of final product obtained in the stir casting by cooling (Air, Furnace and Brine solution) [30] and the third factor was the stirring speed for the proper mixing of aluminum nanocomposites (250, 450 and 650 rpm). Table 5 contains a list of the variables investigated and their associated levels.

3.2. Orthogonal Array

To achieve Taguchi's [32, 34] high efficiency, an orthogonal array is necessary [25–26]. To extract OA from factorial designs of trials, a combination of combinatorics, geometry, finite fields, and error-correcting algorithms is required. The algorithms allow for an OA to be constructed statistically independently, with both levels within a column occurring equally often within the other column, and each level within a column occurring equally often within each other column. As a result, the columns are said to be orthogonal to one another. The amount of interesting elements and interactions, as well as the number of layers for the interesting components, all impact the choice of orthogonal array.

Figure 8. Data of Cumulative Wear Loss of Alloy

Table 5. Factors interested and their levels

Sl. No	Factors	Levels		
		Level - 1	Level - 2	Level - 3
1	% Composition (A)	0.25	0.50	1.00
2	Cooling type (B)	Air Cooling	Furnace Cooling	Brine Solution
3	Stir Speed (C)	250	450	650

 © 2024 Jordan Journal of Mechanical and Industrial Engineering. All rights reserved - Volume 18, Number 4 (ISSN 1995-6665)

This experiment has three parameters, each with three levels. The experiment has a total of six degrees of freedom (DOF) since a three-level parameter has two degrees of freedom (DOF). Orthogonal arrays used in experiments are expected to have a DOF greater than the total DOF of the experiment. Additionally, there cannot be an extreme difference; otherwise, the additional effort and expense of the extra studies are wasted. To study the effects of a set of three to four parameter tiers on L9 orthogonal arrays, the L9 orthogonal array with eight degrees of freedom was chosen. Figure 6 shows the array.

Table 6. L9 Experimental Design

Trial no	Composition % (A)	Cooling (B)	Speed (rpm) (C)
1	0.25	Cooling through air	250
2	0.25	Cooling through furnace	450
3	0.25	Cooling through brain	650
4	0.50	Cooling through air	450
5	0.50	Cooling through furnace	650
6	0.50	Cooling through brain	250
7	1.00	Cooling through air	650
8	1.00	Cooling through furnace	250
9	1.00	Cooling through brain	450

3.3. Wear Rate Test

ANOVA analysis were used to investigate the effect of characteristics such as MWCNT composition, cooling method, and stirring speed. The analysis was conducted with a 95% confidence interval. The signal to noise ratio (S/N ratio) was measured by completing one repetition for each of the nine trials. Pin-on-disc wear testing was conducted on a "DUCOM" machine. Three levels of wear testing were carried out [83]. Dry sliding friction wear testing is used to see how the parameters, such as MWCNT composition, cooling method, and stirring speed, affect the composites wear resistance. The variable "Time" was used in the first step of wear testing, while the variable "slide distance" was used in the second stage.

3.3.1. Wear Rate with Time

Table 6 displays the wear rate over time for each of the nine treatment conditions. We investigated the impact of several parameters on the composites' wear characteristics. The rate of wear is calculated after ten minutes.

3.3.1.1. Wear Rate at 10 Minutes

Table 7 displays the results of a study on the effects of composition, cooling method, and stirring speed on the wear rate of composites with reinforcement levels of 0.25 percent, 0.50 percent, and 1.00 percent and particles with an average size of 40 microns. In this case for 10min the optimal combination was achieved for air cooling with a sliding speed of 650 RPM with aware of 0.004846 µm.

ANOVA was used to determine which variables had a significant effect on the performance metrics. Table 8 summarizes the findings of a 95 percent confidence interval analysis of variance (ANOVA) for the wear. The F-test is based on the idea that the more F a specific process parameter has, the more impact that process parameter change has on the performance characteristic.

The ANOVA results for the wear rate S/N ratio are presented in Table 8, along with the 95 percent confidence interval. In the F test, it was found that the kind of cooling had the greatest impact on wear rate, followed by composition and stirring speed. Table 9 presents a ranking of various elements based on their relative significance. While stirring speed has the lowest rank and was proved to have no influence on wear, the type of cooling has the highest rating, indicating that it makes the biggest contribution to lowering wear. The major effect plot and interaction plot of the S/N ratio for wear rate after 10 minutes are shown in Figures 9 and 10, respectively.

Table 7. Linear Model Analysis: SN ratios versus Composition of MWCNT's (%), Type of cooling, Stirring Speed

Composition of MWCNT's (%)	Type of Cooling	Stirring Speed (rpm)	Wear at 10 minutes (µm)	Mean	S/N Ratio
0.25	A	250	0.005802	0.00582	44.7285
0.25	F	450	0.006719	0.00672	43.4539
0.25	B	650	0.006295	0.00633	44.0201
0.5	A	450	0.005429	0.00543	45.3056
0.5	F	650	0.006528	0.00653	43.7044
0.5	B	250	0.005846	0.00585	44.6628
1	A	650	0.004846	0.00485	46.2923
1	F	250	0.005872	0.00587	44.6243
1	B	450	0.005912	0.00591	44.5653

Table 8. Analysis of Variance (ANOVA) for S N ratios of Wear Rate at 10 minutes

Source	DF	Seq SS	Adj SS	Adj MS	F	P
Composition of MWCNT's (%)	2	1.7989	1.7989	0.89944	5.21	0.161
Type of Cooling	2	3.5855	3.5855	1.79274	10.38	0.088
Stirring Speed	2	0.1062	0.1062	0.05311	0.31	0.765
Residual Error	2	0.3453	0.3453	0.17263		
Total	8	5.8358				

Table 9. (a) Response Table for Means and (b) Response Table for Signal to Noise Ratios

Response Table for Means			
Level	Composition of MWCNT's (%)	Type of Cooling	Stirring Speed
1	0.006272	0.005359	0.00584
2	0.005934	0.006373	0.00602
3	0.005543	0.006018	0.00589
Delta	0.000729	0.001014	0.00018
Rank	2	1	3

Response Table for Signal to Noise Ratios			
Level	Composition of MWCNT's (%)	Type of Cooling	Stirring Speed
1	44.07	45.44	44.67
2	44.56	43.93	44.44
3	45.16	44.42	44.67
Delta	1.09	1.51	0.23
Rank	2	1	3

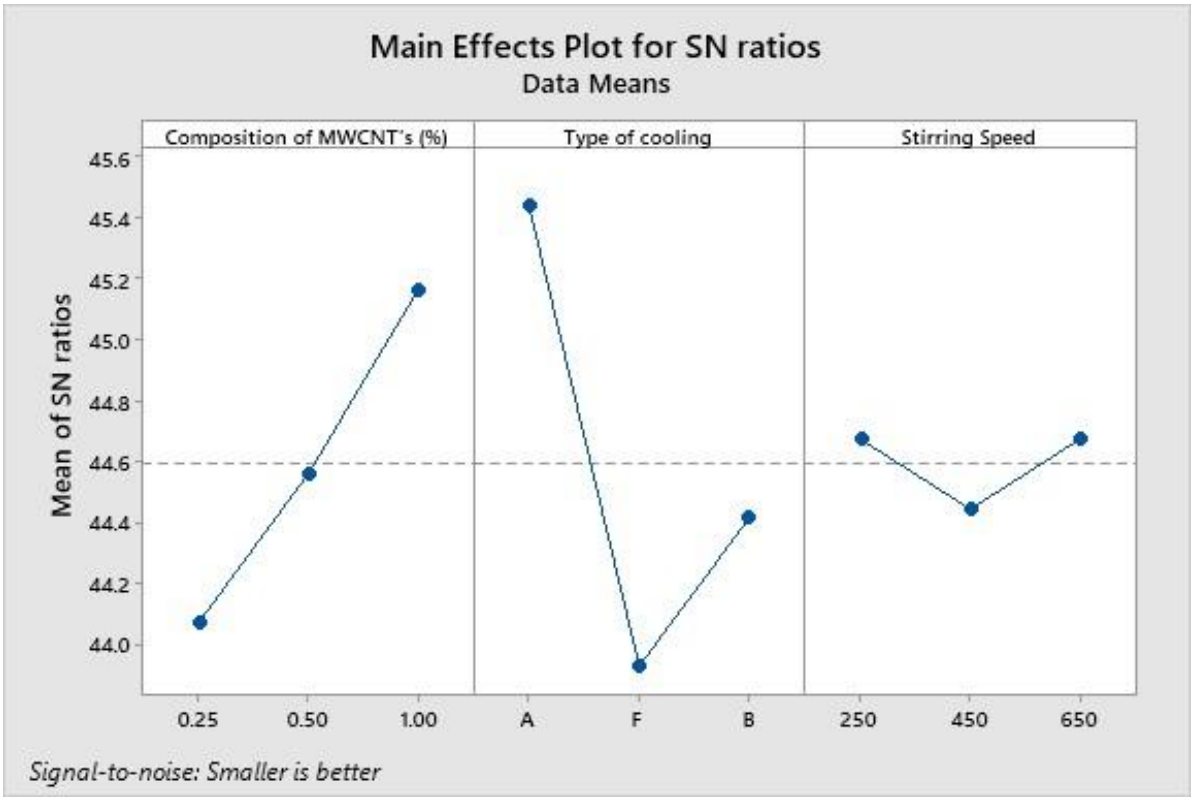

Figure 9: Main Effect Plot for Wear at 10 minutes for SN Ratios

 © 2024 Jordan Journal of Mechanical and Industrial Engineering. All rights reserved - Volume 18, Number 4 (ISSN 1995-6665)

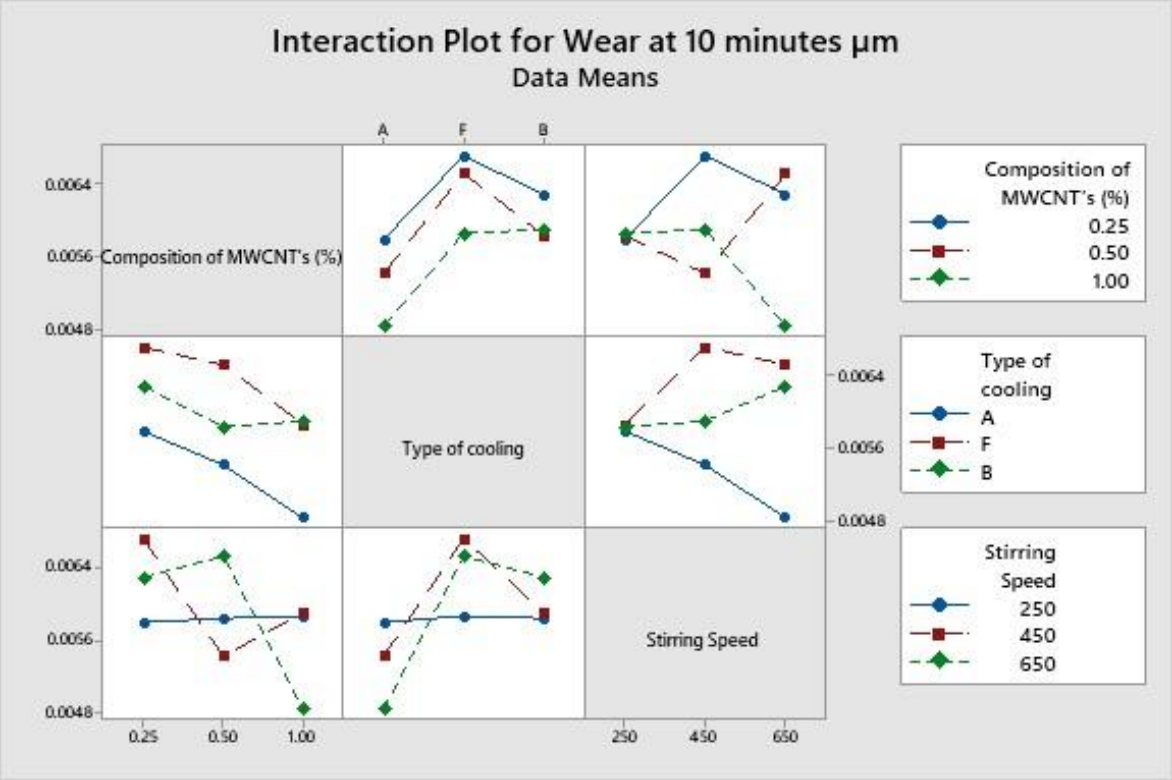

Figure 10. Interaction Plot for Wear at 10 minutes for SN Ratios

Table 10. Significant factors for wear rate at 10 minutes of composites

Factors	Affecting mean		Affecting variation (S/N ratio)	
	Contribution	Best level	Contribution	Best level
Composition (A)	Significant	Level 3 - 0.5%	Significant	Level 3 – 0.5%
Cooling (B)	Significant	Level 3 - FC	significant	Level 3 - FC
Stirring Speed (C)	Insignificant	-	Insignificant	-

3.3.1.2. Results of Wear Rate with Time

The influence of numerous characteristics on the wear rate of composites formed by L9 treatment was investigated using ANOVA. These parameters included composition, cooling, and stirring speed. At 10-, 20-, and 30-minute intervals, the wear rate was determined. The following graphs for means and S/N ratios were used to compare the effect of the adjustments. Significant parameters have a "P" value less than 0.20, whilst those with a "P" value more than 0.20 are not. The response table is used to rank the different factors according to how they affect wear rate. The two parameters, composition and cooling type, were shown to be important at each time, while the parameter stirring speed was inconsequential.

According to Table 10, for composition level 3, "0.50 percent" was always the best option in every situation, and for cooling, "furnace cooling" was always the greatest option in every situation. However, when all of the data were taken into account, furnace cooling won. The parameter stirring speed was inconsequential at all times. In comparison to air cooling and furnace cooling, the structure formed during furnace cooling is denser. The addition of MWCNT particles during cooling increases the bonding strength of the AMNCs, resulting in a decrease in wear rate. The MWCNT particles' higher strength contributes to a decrease in wear rate. When the AMNC wear rate is compared to the passage of time, the wear rate rises over time.

3.3.2. Wear Rate with Sliding Distance

Upon performing a wear behavior analysis over time, the sliding distance wear rate was ascertained. On the basis of 1000-meter sliding distances, the wear rate was evaluated. Additionally, the effect of variables on the wear rate vs sliding distance was investigated, including the composition of MWCNT, the cooling technique, and the stirring speed. The wear rate was calculated using equations (2), (3), and (4) based on the decrease in pin height during the performance testing.

3.3.2.1. Wear Rate at 1000 Sliding Distance (µm)

Table 11 shows how composition, cooling method, and stirring speed affect the wear rate of composites having 0, 25, 0, and 1 percent reinforcing particles with an average size of 40 microns.

The data underwent ANOVA analysis [28] to determine the variables significantly impacting the performance indicators. Table 12 displays the 95 percent confidence interval for the ANOVA results regarding the S/N ratio of

the wear rate. The F-test operates under the principle that higher F values for specific process parameters indicate a more pronounced influence of those parameter changes on the performance characteristic. The kind of cooling was shown to be the most important element influencing the wear rate in the F-test, followed by composition and stirring speed. Table 13 presents a ranking of the relative significance of the major elements. Although stirring speed was found to have no impact on wear and holds the lowest rank, the type of cooling received the highest rating, suggesting that it makes the most significant contribution to reducing wear. Figures 11 and 12 illustrate the interaction plot and main effect plot, respectively, of the S/N ratio for wear rate after 1000 sliding distances (m). In this case for 1000 sliding distance the optimal combination was achieved for water cooling with a stirring speed of 250RPM with a wear of 0.486010 µm

Table 11. Linear Model Analysis: SN ratios versus Composition of MWCNT's (%), Type of cooling, Stirring Speed

Composition of MWCNT's (%)	Type of Cooling	Stirring Speed (rpm)	Wear at 1000 sliding distance µm	Mean	S/N Ratio
0.25	A	250	0.785874	2.092941585	0.785874
0.25	F	450	0.628274	4.037018248	0.628274
0.25	B	650	0.690707	3.214122852	0.690707
0.5	A	450	0.758941	2.395839696	0.758941
0.5	F	650	0.563754	4.978207273	0.563754
0.5	B	250	0.643983	3.822511942	0.643983
1	A	650	0.689952	3.223622442	0.689952
1	F	250	0.486019	6.266935053	0.486019
1	B	450	0.595711	4.499287609	0.595711

Table 12. Analysis of Variance (ANOVA) for S N ratios of Wear Rate at 1000 Sliding Distance (µm)

Source	DF	Seq SS	Adj SS	Adj MS	F	P
Composition of MWCNT's (%)	2	3.6464	3.6464	1.82318	34.14	0.028
Type of Cooling	2	9.5505	9.5505	4.77527	89.41	0.011
Stirring Speed	2	0.2650	0.2650	0.13248	2.48	0.287
Residual Error	2	0.1068	0.1068	0.05341		
Total	8	13.5687				

Table 13. (a) Response Table for Means and (b) Response Table for Signal to Noise Ratios

(a) Response Table for Means

Level	Composition of MWCNT's (%)	Type of Cooling	Stirring Speed
1	0.7016	0.7449	0.6386
2	0.6556	0.5593	0.6610
3	0.5906	0.6435	0.6481
Delta	0.1111	0.1856	0.0224
Rank	2	1	3

(b) Response Table for Signal to Noise Ratios

Level	Composition of MWCNT's (%)	Type of Cooling	Stirring Speed
1	3.115	2.571	4.061
2	3.732	5.094	3.644
3	4.663	3.845	3.805
Delta	1.549	2.523	0.417
Rank	2	1	3

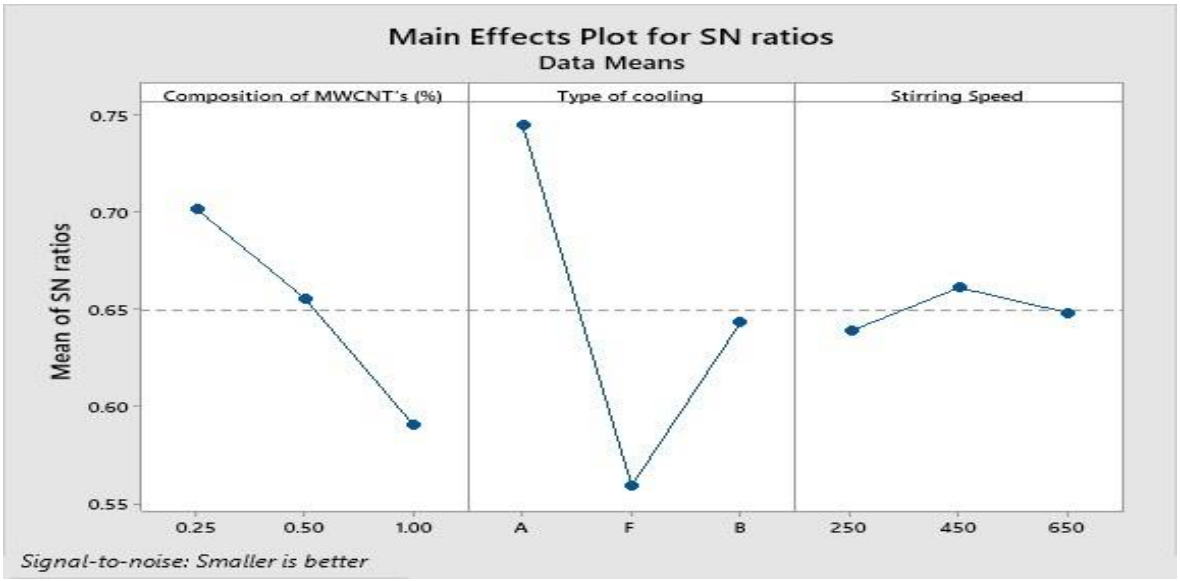

Figure 11: Main Effect Plot for Wear at 1000 Sliding Distance (µm) for SN Ratios

 © 2024 Jordan Journal of Mechanical and Industrial Engineering. All rights reserved - Volume 18, Number 4 (ISSN 1995-6665)

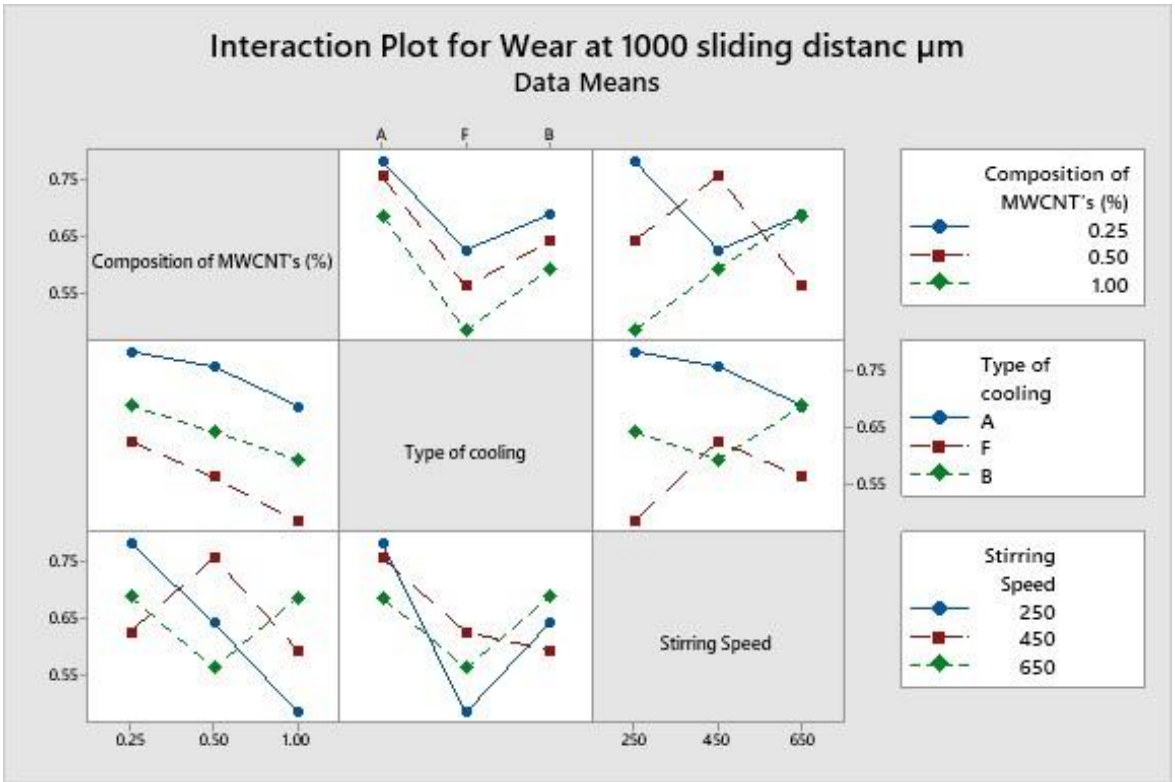

Figure 12. Interaction Plot for Wear at 1000 Sliding Distance (µm) for SN Ratios

3.3.2.2. Results of Wear Rate with Sliding Distance

ANOVA was employed to assess the impact of multiple factors, including composition, cooling, and stirring speed, on the wear rate with sliding distance in composites formed through L9 treatment. To assess the significant and insignificant components, mean and S/N ratio plots were utilized to compare the parameters. ANOVA's "P" value was utilized to identify which parameters were statistically significant and which were not. Significant variables have a "P" value less than 0.05, while insignificant factors have a "P" value greater than 0.05. The two factors cooling and composition were found to be significant variables in determining the sliding distance, however the parameter stirring speed was not, when the mean values and S/N ratios were compared. The composition study's findings for sliding distances, i.e. for sliding distance 1000, showed that the level 3 experienced significant cooling, or "furnace cooling," in the case of composition. In the case of cooling, the findings for sliding distances, i.e. for sliding distance 1000, indicated that the substantial cooling was at level 3, or "furnace cooling."

The resulting wear rate wasn't linearly proportional to applied force when the composite wear rate was compared to the sliding distance. When a load is applied, two distinct forms of wear behavior may be expected. Samples on sliding discs are abrasive, resulting in debris, the wear was initially unstable and variable. In the case of composites, the wear rate first rises and then gradually decreases as sliding distances grow. The MMC is softer at the beginning of the sliding process than it is at the end because, after a given number of sliding distances, the MMCs become strain hardened as a result of continuous sliding under the applied force.

4. Worn Surfaces for Microstructure analysis

As shown in Figure 13(a-h), the specimens' worn-out surfaces are examined using a SEM at different weight percentages of MWCNTs while adhering to a constant applied force of 20 N, sliding speed of 2.5 m/s, and sliding distance of 1000 m. Furthermore, SEM micrographs are examined to evaluate the impact of MWCNTs on the fabricated AMNCs specimens' wear behavior. The SEM micrographs demonstrate the compositional homogeneity in the images. Even so, microstructural analysis of some worn-out surfaces revealed the presence of MWCNT nanoparticles there (c - f). Microscopic inspection reveals that the MWCNTs' presence and the homogeneity of their distribution inside the matrix are what contribute to the increased wear resistance. Particle cracking and severe debonding cause surface failure. Broken nanoparticles were undoubtedly entrapped in an Al ductile matrix, revealing moderately worsened wear loss. Surface adhesion causes adhesive or sliding wear (c). Contact asperities smooth each other out, resulting in a fracture on one of the faces. SEM images of the crack and the sticky zone can be seen in a variety of ways. Furthermore, adhesive wear might be depicted as minor damage plastically deforming within the surface stratum. Oxide particles are created when oxygen and iron or aluminium combine chemically. The tremendous heat created between the surfaces during the wear test results in the formation of black oxides on the worn surfaces (g). Figure 13 illustrates the effects of detachable adhesion debris and substantial surface debris on the worn surfaces of Al as-cast (a & b) and AMNCs, which include scratches, cracks, delamination, sliding wear plastic deformation, and many cavities (a-h). However, as illustrated in figure 13, significant heat generation causes

severe damage, cracks, and grooves (c- h). The plastic flow marks are visibly visible. It supports the presence of Al as-cast and AMNCs with severe plastic deformation. The additional heat created between the surfaces causes a reduction in shear strength. Similar to this, before the sample is transmitted to the disc, the higher material is extracted from it. Research has been conducted to explore the origins of delamination wear and variations in wear severity, ranging from minor to severe. The findings unveiled that, when subjected to a consistent load of 20 N and varying speeds from 3 to 12 m/s, the worn surfaces of the composite displayed a noticeable black adhering layer mainly comprising friction material components. This layer acted as a protective coating and lubricant, significantly augmenting the wear resistance of the composites.

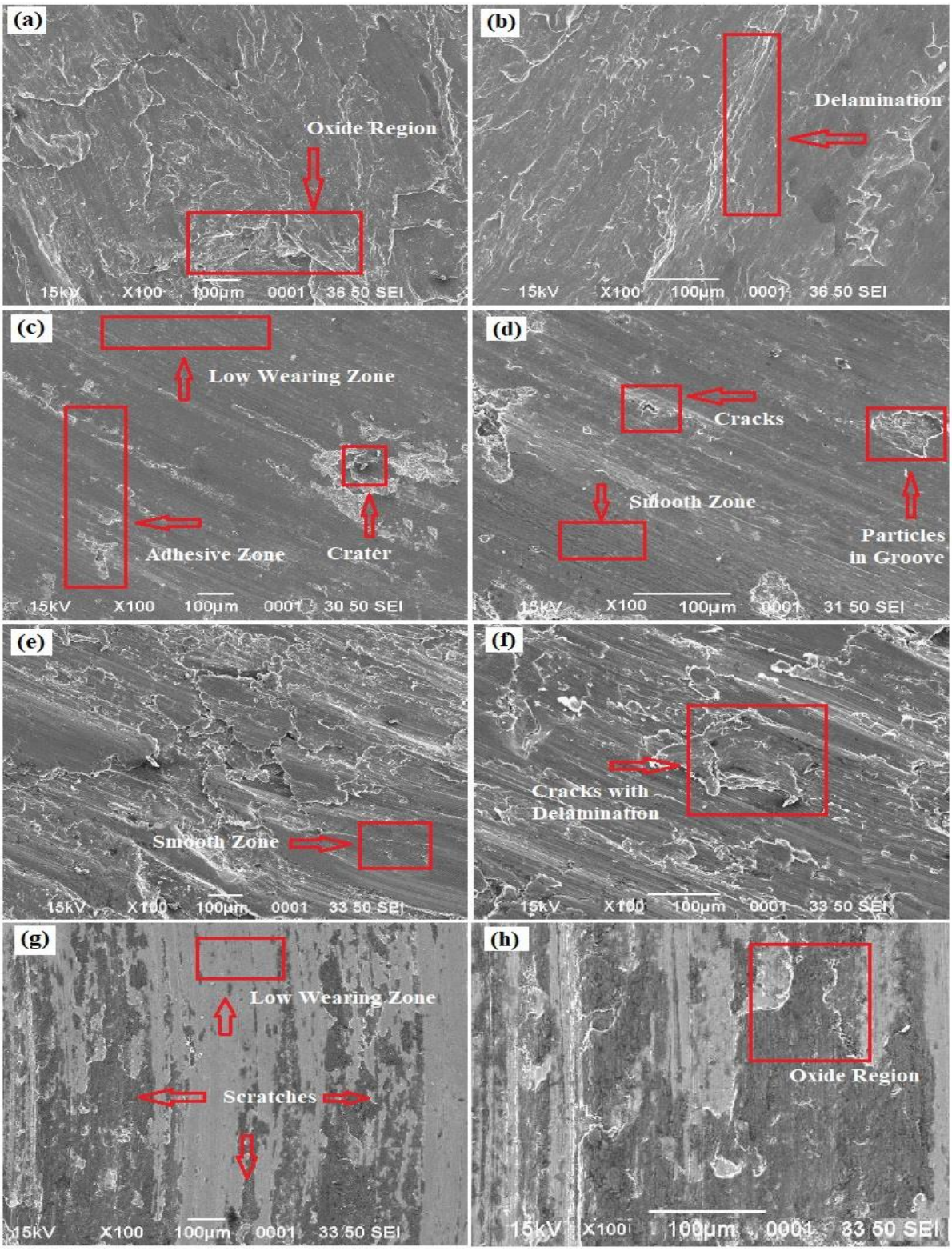

Figure 13. SEM micrographs of worn surface at 20 N load, speed 2.5 m/s and 1000 m distance: (a) and (b) As-cast LM29, (c) and (d) LM29 + 0.25% MWCNT's, (e) and (f) LM29 + 0.50% MWCNT's, and (g) and (h) LM29 + 1.00% MWCNT's

 © 2024 Jordan Journal of Mechanical and Industrial Engineering. All rights reserved - Volume 18, Number 4 (ISSN 1995-6665)

4.1. ANN Modeling

In order to anticipate the wear as an output, the current work used an MLPNN model, which is a feed forward-backward propagation artificial neural network, taking into account two input parameters, such as composition (MWCNT) and stirring speed (Fig. 14). The input layer, hidden layer, and output layer are the three layers that make up the model's structure and show the Eq. 5 (23). The model [31, 33, 35] was created using a multilayer perceptron neural network model, which has ten neurons and provides the best result for all combinations examined. When there is wear, the MSE output value for two inputs is -0.26358 (Fig. 15). During the training process, the input parameters enter the feed forward neural networks is given in Eq.5 (23) each product of input parameters (M_i) and a weight function (W_{ij}) are summed into the junction and is summed with bias (b_j) of the neurons as follows.

$$X = \left(\sum_{i=1}^{n} \left(W_{ij} M_i\right)\right) + b_j \quad (5)$$

The input parameters enter the feed forward neural networks during the training and testing process, as illustrated in Figure 14. Each product of input parameters (Mi) and a weight function (Wij) is summed into the junction and is summed with the neurons' bias (bj) in the manner as follows (Eq. 5). The input factors, including compositions and stirring speed, were taken into consideration in this inquiry. In a similar vein, wear is taken into account. In the end, models for predicting performance were created for each and every output parameter that was taken into account. Finally, Fig. 16 displays the data for training and total performance. The predicted and the measured values clearly show that there is a 95% of confidence between the ANN and the data extracted from the experimental investigations (Fig 16, 17 and 18). Hence the predicted data using ANN [29] with 10 neurons gave a better result with acceptable accuracy of more than 95% (Table 14).

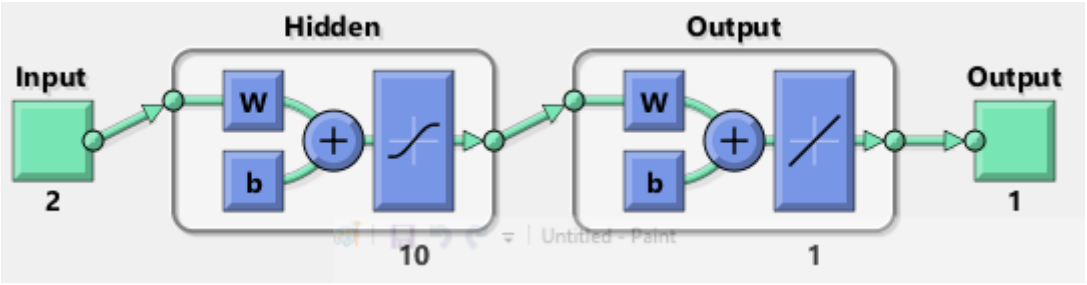

Figure 14. Developed Network for two input with one output variable (Wear for 10 minutes)

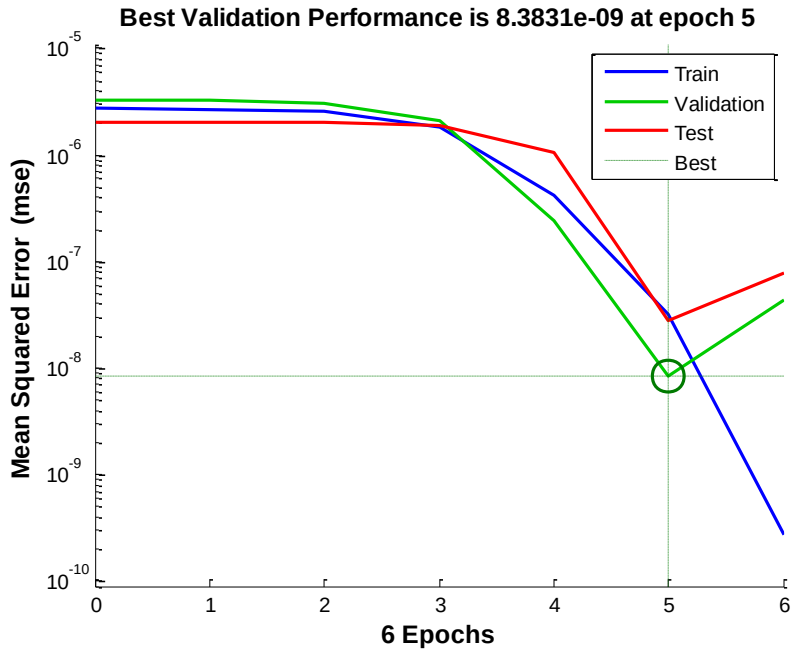

Figure 15. Mean Square error for all combinations of MWCNT with different stirring speed (Wear for 10 minutes)

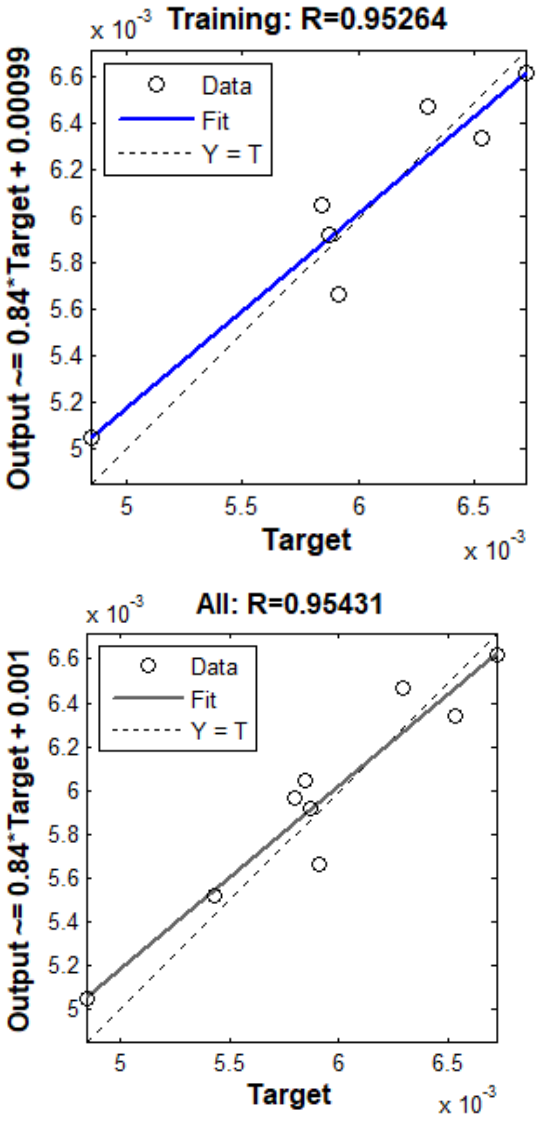

Figure 16. Training and the overall results for all combinations considered (Wear for 10 minutes)

Table 14. Weights and bias of the optimum model (2-5-1) one outputs (Wear)

Weights between the input and hidden layer (W_{2*5})	
2.7523	0.84081
-2.97	-0.74672
-0.4847	-3.1344
2.9484	-0.61069
-0.08816	3.1531
Bias in hidden layer (B_{1*5})	
[-3.4026, 1.6531, -0.13132, 1.8154, -3.1073]	
Weights to output layer (W_{1*5})	
[-0.8391, 0.078619, 0.066819, -0.32237, 0.2282]	
Bias in output layer (B_{1*1})	
[-0.26358]	

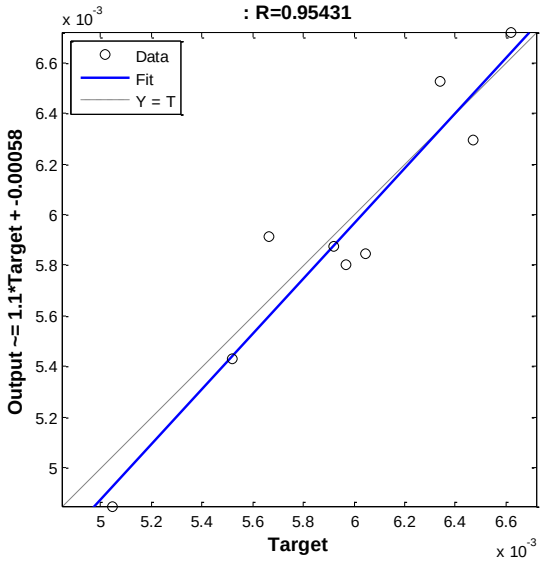

Figure 17. Predicted and measured data for all the combinations considered.

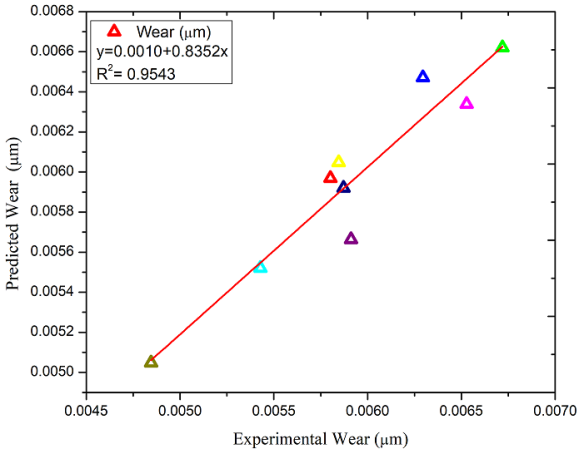

Figure 18. Predicted and experimental values for wear for 10 minutes' run

5. Comparative analysis

Comparison of the experimental, statistical and predicted data for LM29 is determined. Based on the observations, all three different performance data is shown in Fig. 19. From the comparative graphs, it clearly shows that the difference between all the three data sets are less than 5% and predictive capability found to be in the acceptable range with the experimental data sets. Finally, it states that the analyses are within the limit with 95% confidence interval with better performance to predict the wear rate of LM29 for different combinations considered.

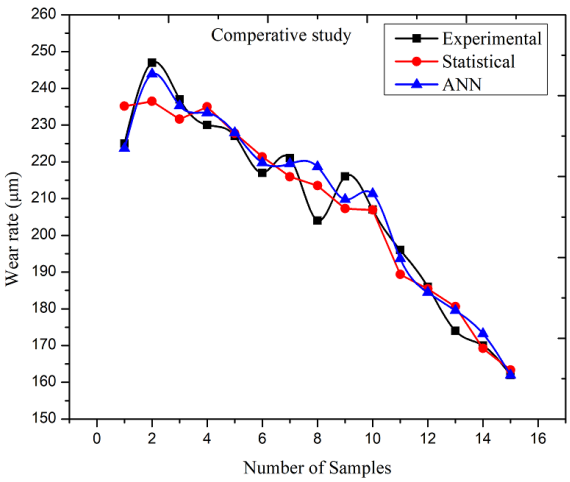

Figure 19. comparative study of all the three different study of LM29

6. Conclusion

Stir casting was used to create aluminum matrix nanocomposites (LM29/MWCNTs) utilizing the Liquid Metallurgy Route. The Taguchi and ANOVA parameter designs were shown to provide a straightforward, systematic, and efficient way for optimizing process parameters. For minimum wear loss, the ideal set of factor levels was found to be 0.5 wt. percent MWCNT reinforcement concentration, furnace cooling type, 1000 m sliding distance, and 20 N applied load. The effect of type of cooling has the highest percent contribution (10.38%) for the analysis of wear rate at 10 minutes, followed by reinforcement concentration (89.41%), and the effect of type of cooling has the highest percent contribution (34.41%) for the analysis of wear rate at 1000 m sliding distance, followed by reinforcement concentration (5.21%). Additionally, it was revealed that stirring speed was irrelevant at the 5% level of significance, although concentration and the kind of cooling were both shown to be significant. The presence of MWCNTs and their uniformity in the matrix are responsible for increasing wear resistance, according to microscopic inspection of worn surfaces. The bulk of the time, SEM micrographs were employed to demonstrate the homogeneity of the MWCNTs. It was discovered that AMNCs had lesser distorted region penetration than the LM29 as-cast sample. Craters, grooves, and fissures appeared on worn-out surfaces as a result of delamination of surfaces and scratching of surfaces. Furthermore, SEM predicted oxide layers on worn surfaces. The ANN models that were constructed have an RMSE value of 8.3839*10-9 for wear. For five neurons with two input parameters, the performance prediction model was therefore optimal. The R2 (VAF) was therefore 0.9543.

REFERENCES

[1] Roger Lumley, Fundamentals of Aluminium Metallurgy: Production, Processing and Applications, Woodhead Publishing Series in Metals and Surface Engineering, Elsevier, 2010

[2] S. Basavarajappa, G. Chandramohan, J. Paulo Davim, “Application of Taguchi techniques to study dry sliding wear behavior of metal matrix composites”, Materials and Design, 28, 2007, pp. 1393-1398.

[3] S. Basavarajappa, G. Chandramohan, J. Paulo Davim, “Application of Taguchi techniques to study dry sliding wear behaviour of metal matrix composites”, Materials and Design, 28, 2007, pp. 1393-1398.

[4] G.P. Prasad, H.C. Chittappa, M. Nagaral, V. Auradi, Effect of the reinforcement particle size on the compressive strength and impact toughness of LM29 alloy-B4C composites. Struct. Integrity Life 19(br. 3), 231–236 (2019)

[5] Hernandez FCR, Sokolowski JH (2006) Thermal analysis and microscopical characterization of Al–Si hypereutectic alloys. J Alloys Compd 419:180–190

[6] Sha M, Wu S, Wan L (2012) Combined efects of cobalt addition and ultrasonic vibration on microstructure and mechanical properties of hypereutectic Al–Si alloys with 0.7% Fe. Mater Sci Eng A 554:142–148

[7] Hekmat-Ardakan A, Ajersch F (2010) Thermodynamic evaluation of hypereutectic Al–Si (A390) alloy with addition of Mg. Acta Mater 58:3422–3428

[8] Vijeesh V, Prabhu KN (2014) Computer aided cooling curve analysis and microstructure of cerium added hypereutectic Al–Si (LM29) alloy. Trans Indian Inst Met 67:541–549

[9] Vikram Kedambadi Vasu and Dr. Umashankar K S, Experimental Investigation of Multi-Walled Carbon Nanotubes Dispersion on Mechanical Properties of Aluminum-Silicon Alloys (Lm6 And Lm25) by Stir Casting Method, International Journal of Mechanical Engineering and Technology 8(8), 2017, pp. 341–348. http://iaeme.com/Home /issue /IJMET?Volume=8&Issue=8

[10] V.P. Patel, H.R. Prajapati , Microstructural and mechanical properties of eutectic Al - Si alloy with grain refined and modified using gravity die and sand casting, IJERA, Vol. 2, Issue 3, (2012) 147-150.

[11] Satya Prema, Murali G.E, T.M. Chandrashekharaiah, Studies of Microstructures and Mechanical Properties on Al-Si Alloy(A390) using Grain refiners and/or Modifier, International Journal of Scientific & Engineering Research, Volume 7, Issue 8, August-2016, 580 ISSN 2229-5518

[12] Devappa, T.M. Chandrashekharaiah, Studies on the Effect of Minor Addition of Sr and Mg on the Microstructure and Mechanical Properties of A413 Alloy, International Journal of Engineering Research & Technology (IJERT) ISSN: 2278-0181, IJERTV4IS060032, Vol. 4 Issue 06, June-2015

[13] Bharath V., Nagaral M., Auradi V., Kori S. A., Preparation of 6061 Al- Al_2O_3 MMC's by Stir Casting and Evaluation of Mechanical and Wear Properties, Procedia Materials Science, 2014, 6:1658-67

[14] Rana R. S., Rajesh Purohit and Das S., Reviews on the Influences of Alloying elements on the Microstructure and Mechanical Properties of Aluminium Alloys and Aluminium Alloy Composites, International Journal of Scientific and Research Publications, Vol.2, Issue 6, June 2012

[15] Angadi B. M., Chennakesava Reddy A., Auradi V., Nagathan V.V., Kori S.A., Effect of Al-5Ti-B Addition on Microstructure, Mechanical and Thermal Properties of Hypereutectic Al-20Si Alloy, International Conference on Advanced Material Technologies – 2016, 27th and 28th December 2016

[16] Satya Prema, T.M. Chandrashekharaiah, Farida Begum P., Effect of Grain Refiners and/or Modifiers on the Microstructure and Mechanical Properties of Al-Si Alloy (LM6), Materials Science Forum, ISSN: 1662-9752, Vol.969, pp 794-799 (2019)

[17] Satya Prema, T.M. Chandrashekharaiah, Farida Begum P., Study of Improvement in Mechanical Properties and Microstructure of LM25 Alloy with the Addition of Grain

Refiners / Modifier, International Journal of Applied Engineering Research, ISSN:0973-4562, Vol.14, No.6, (2019) pp. 1297-1300

[18] Satya Prema, T.M. Chandrashekharaiah, Srinivasa Murthy M.K., Statistical Analysis of Ultimate Tensile Strength of Grain Refined and Modified Al-Si Alloys (LM-25, LM-6 and LM-30) Using ANOVA, International Journal of Scientific & Engineering Research, Volume 12, Issue 2, February-2021 160 ISSN 2229-5518

[19] Kakria, Ravneet and Singh, Chandandeep and Thareja, Priyavrat, Quality Improvement of Aluminum Alloy (LM-6) Casting Using Taguchi Method (2007). Indian Foundry Journal, November 2007, http://dx.doi.org/10.2139/ssrn.1487542

[20] Sangeeth kumar, E., et al. (2019) Tribological Study on Hybrid Metal Matrix Composites for Application in Automotive Sector. Materials Research Express, 6, Article ID: 055703. https://doi.org/10.1088/2053-1591/ab0579

[21] S.C. Sharma, M. Krishna, A. Shashishankar, S. Paul Vizhian, "Damping behavior of aluminium/short glass fibre composites", Materials Science and Engineering A364 (2004)109–116.

[22] Varna K, Vijay Kumar S, Lakshmidevamma M M, Benal M M, "Prediction of Temperature during machinability of Al2O3 reinforced Al7075", Journal of Composite and Advanced Materials, International Information and Engineering Technology Associations, Vol. 30 (5-6), 241-246.

[23] Vijay Kumar S, B. M. Kunar, Ch. S. N. Murthy, "ANN model for prediction of bit-rock interface temperature during rotary drilling of limestone using embedded thermocouple technique", Journal of Thermal Analysis and Calorimetry, Vol. 139 (3), 2020, pp. 2273-2282.

[24] Vijay Kumar S, B. M. Kunar, Ch. S. N. Murthy, M. R. Ramesh "Measurement of bit-rock interface temperature and wear rate of the tungsten carbide drill bit during rotary drilling", Friction. Vol. 8 (6), pp. 1073-1082.

[25] Vijay Kumar S, B. M. Kunar, Ch. S. N. Murthy, "Experimental investigation and statistical analysis of operational parameters on temperature rise in rock drilling", International Journal of Heat and Technology. Vol. 36 (4) 2018, pp. 1174-1180.

[26] Vijay Kumar S, Ch. S. N. Murthy, B. M. Kunar, "Effect of thermal response on physical properties during drilling operations-A case study", Materials Today, Vol. 5 (2) 2018, pp. 7404-7409. (SCOPUS).

[27] Vardaraj K R, Vijay Kumar S, Manjunath C, M Ravi Kumar, "Study the impact of operational parameters on interface temperature during rotary drilling", Materials Today. Vol. 45 (1), 2021, pp 412-414.

[28]Ravikumar M, Hanumanthe Gowda, Vijay Kumar S, Reddappa H N, Suresh R, "Study on Strontium and Sodium Modification Elements on Microstructure, Mechanical, Wear and Fracture Behavior of Al7075 Alloy by Taguchi Technique", Jordan Journal of Mechanical and Industrial Engineering. Vol. 18 (1), 2024, pp 145- 157.

[29] Parashuram A Kutakanakeri, K. Rama Narasimha, K. Gopalakrishna, Laxminarayana K.G Bhatta, "Radial basis Neural Network Model to Prediction of Thermal Resistance and Heat Transfer Coefficient of Oscillating Heat Pipe Using Graphene and Acetone-Based Nanofluids", Jordan Journal of Mechanical and Industrial Engineering. Vol. 18 (2), 2024, pp 251- 266.

[30] Vikram K Vasu, Umashankar K S, Vijay Kumar S, "Empirical Analysis of Multiwalled Carbon Nanotube Deposition for Enhancing Mechanical and Tribological Characteristics in Aluminium-Based Metal Matrix Composites", Jordan Journal of Mechanical and Industrial Engineering. Vol. 17 (4), 2023, pp 471– 480.

[31] Ayman Alkhatatbeh, Mohammad A Gharaibeh, Rami Al-Jarrah, Ali M. Jawarneh, "Artificial Neural Networks Modeling of the Electricity Demands in the Jordanian Industrial Sector", Jordan Journal of Mechanical and Industrial Engineering. Vol. 18 (2), 2024, pp 297- 309.

[32] Talal Alsardia, Dr. László Lovas, "Investigation of the Effect of the Surface Treatment and Lubrication During Repeated Tightening on the Nut Coefficient of a Bolted Joint Using the Taguchi Method", Jordan Journal of Mechanical and Industrial Engineering. Vol. 18 (1), 2024, pp 131- 144.

[33] Tallal Hakmi1, Amine Hamdi, Aissa Laouissi, Hammoudi Abderazek, Salim Chihaoui, Mohamed Athmane Yallese, "Mathematical Modeling Using ANN Based on k-fold Cross Validation Approach and MOAHA Multi-Objective Optimization Algorithm During Turning of Polyoxymethylene POM-C", Jordan Journal of Mechanical and Industrial Engineering. Vol. 18 (1), 2024, pp 179- 190.

[34] Hany Mohamed Abdu, Sayed M. Tahaa, A.Wazeer, A.M.Abd El-Mageed, Moustafa M. Mahmoud, "Application of Taguchi Method and Response Surface Methodology on Machining Parameters of Al MMCs 6063-TiO_2", Jordan Journal of Mechanical and Industrial Engineering. Vol. 17 (4), 2023, pp 489– 499.

[35] Sovan Bhowmicka, Binod Baraia, Debismita Naikb, Subhasish Sarkara, Nisantika Biswasc, Swapan Kumar Maityd, Gautam Majumdara, "Parametric Study and Optimization of Inconel 625 Processing by ANN and Desirability Function Approach During Graphite Mixed EDM", Jordan Journal of Mechanical and Industrial Engineering. Vol. 17 (4), 2023, pp 625– 643.